

Identification of 2H and 3R polytypes of MoS₂ layered crystals using photoluminescence spectroscopy

S. Anghel,^{1,2} Yu. Chumakov,¹ V. Kravtsov,¹ A. Mitioglu,^{1,3} P. Plochocka,³ K. Sushkevich,⁴ G. Volodina,¹ A. Colev,¹ and L. Kulyuk¹

¹*Institute of Applied Physics, Academiei Str. 5, Chisinau, MD-2028, Republic of Moldova*

²*Ruhr-Universität Bochum, Anorganische Chemie III, D-44801 Bochum Germany**

³*LNCMI, CNRS-UJF-UPS-INSA, Grenoble and Toulouse, France*

⁴*State University of Moldova, Mateevici Str. 60, Chisinau, MD-2009, Republic of Moldova*

(Dated: November 17, 2014)

The excitonic radiative recombination of intercalated Cl₂ molecules for two different polytypes 2H-MoS₂ and 3R-MoS₂ layered crystals are presented. The structure of the excitonic emission is unique and provides a robust experimental signature of crystal polytype investigated. This result is confirmed by X-ray diffraction analysis and DFT electronic band structure calculations. Thus, the bound exciton emission provides a nondestructive fingerprint for the reliable identification of the polytype of MoS₂ layered crystals.

I. INTRODUCTION

Transition metal dichalcogenides (TMDC) is an emerging class of materials with an extremely wide spectrum of potential applications, ranging from optoelectronic devices, field effect transistors and solar cell convertors to more mundane lubricants.^{1–4} Single layers of TMDC were first obtained by mechanical exfoliation.⁵ Due to their truly 2D character single layer TMDC's have attracted considerable attention as strong potential candidates for the next generation of electronic devices. However, for future applications the quality of the atomically thin crystals is extremely important.

In order to achieve the required high quality, the control of the synthesis of single crystals is crucial. Among the different methods used to obtain single crystal, chemical vapor transport (CVT) method is widely used with a view to device fabrication. In this method, halogen molecules are used as a transport agent.^{6–8} When synthesizing MoS₂ it is possible to obtain hexagonal (2H), as well as, rhombohedral (3R) polytype layered crystals which have quite different physical properties. For example, the 3R polytype of MoS₂, due to the non-centrosymmetric structure present in this form, exhibits a valley polarization in photoluminescence emission even for a bulk crystal.⁹ To date the electronic properties of 3R phase remain largely unexplored. Clearly, the development of an experimental probe to distinguish the polytype “*in situ*” is essential, especially since traditional Raman spectroscopy appears to be incapable of distinguishing between the 3R or 2H crystal polytype.

In this paper we show that the photoluminescence spectra of excitons bound to halogen molecules^{10–12} in the van der Waals gap of the crystals provide a unique fingerprint for the crystal polytype. X-ray analysis of the crystal structure and density functional theory (DFT) calculations of electronic band structure of the layer type models of MoS₂ have been performed to support our findings.

II. SAMPLE CHARACTERIZATION

The synthetic 2H and 3R-MoS₂ single crystals have been grown by the vapor transport method, using Mo and S as starting materials. The MoCl₅ compound, which decomposes at high temperatures, was used as a source of Cl₂ molecules for the CVT. The starting materials were placed in evacuated sealed quartz ampoules which were slowly heated up to the synthesis temperature of 1150°C for two days and maintained under these conditions for two days more. Subsequently, the ampoules with the polycrystalline material were placed in a two-zone tube furnace. The temperature of the crystallization chamber was set at around 930°C in the region of the crystals growth, according to references [13 and 14]. The two polytypes were obtained by choosing a different temperature gradient and a different concentration of the transport agent, which seems to have an important influence on the growth process. The ampoules were held inside the furnaces for a period of up to 6 days, after which they were slowly cooled to room temperature.

The 2H- and 3R- polytypes were identified and structurally characterized by the single crystal X-ray method. The polymorphic purity of the as synthesized 2H- and 3R-polytypes (bulk samples) was confirmed by comparing the calculated and experimental X-ray powder diffraction patterns. The X-ray diffraction data were obtained at room temperature using an *Xcalibur E* diffractometer. The data were collected and processed using the program CrysAlisPro and were corrected for the Lorentz and polarization effects and absorption¹⁵. The structure was refined by the full matrix least squares method on F^2 with anisotropic displacement parameters using the program SHELXL.¹⁶ The unit cell parameters for 2H-MoS₂ are $a=b=3.1625(1)\text{\AA}$, $c=12.300(1)\text{\AA}$ and for 3R-MoS₂ $a=b=3.1607(7)\text{\AA}$, $c=18.344(9)\text{\AA}$, and the corresponding atomic coordinates are listed in Table I. These parameters are in good agreement with those reported in reference [17] which allows us to conclude that the intercalation with Cl₂ molecules does not change the pa-

2H-MoS ₂				
	<i>X</i>	<i>y</i>	<i>Z</i>	<i>U_{eq}</i>
Mo	1/3	2/3	0.25	6(1)
S	1/3	2/3	6228(1)	7(1)
3R-MoS ₂				
	<i>X</i>	<i>y</i>	<i>Z</i>	<i>U_{eq}</i>
Mo	0	0	0	12(1)
S1	0	0	2490(3)	11(1)
S2	0	0	4189(3)	9(1)

TABLE I. Atomic coordinates 10^4 and equivalent isotropic displacement parameters ($\text{\AA}^2 \times 10^3$). U_{eq} is defined as one third of the trace of the orthogonalized U_{ij} tensor.

rameters of the crystal structure.

III. PHOTOLUMINESCENCE MEASUREMENTS

The PL spectra, recorded using a standard lock-in technique, were excited by the second harmonic emission of a cw-operating YAG: Nd ($\lambda = 532\text{nm}$). The samples were placed in a closed cycle cryostat operating in the temperature range 10 – 100K and the PL emission was collected from the 001 plane of the crystal (parallel to the *c*-axis).

Representative PL spectra measured on the 3R and 2H polytypes of MoS₂ single crystals at $T = 25\text{K}$ are presented in Fig. 1. The emission spectra of 2H and 3R polytypes are marked by red solid and blue broken lines respectively. Each spectrum exhibits several sharp lines. The two strong lines in the energy range 1.17 – 1.19 eV correspond to the two zero-phonon excitonic lines. We label them *B* and *C* following our previous notation.¹¹ The lower energy part of the spectrum is dominated by their phonon replicas where *ph1-ph3* symbols refer to the number of the phonon replica. An analysis of the phonon replica sideband lines leads to the following three values of phonon energy modes: $E_{ph1}=23.9\text{meV}$, $E_{ph2}=28\text{meV}$, and $E_{ph3}=32.1\text{meV}$. To the best of our knowledge this is the first observation of halogen bound exciton emission in the case of the 3R-polytype. Fig. 2 shows an expanded view of PL spectra of the two polytypes measured at different temperatures. Although, the structure of the spectrum for both polytypes is clearly similar, the emission the same excitonic complexes appears at significantly different energies. For example, the 3R emission occurs at an energy 3.5 meV (for *B* exciton) and 6 meV (for *C* exciton) lower than for 2H emission. The resulting energetic separation of the excitonic lines is 10.3 meV for the 3R crystal and only 7.6 meV for the 2H crystal. Thus, the size of the splitting provides a unique fingerprint for each polytype which also has the advantage that it does not

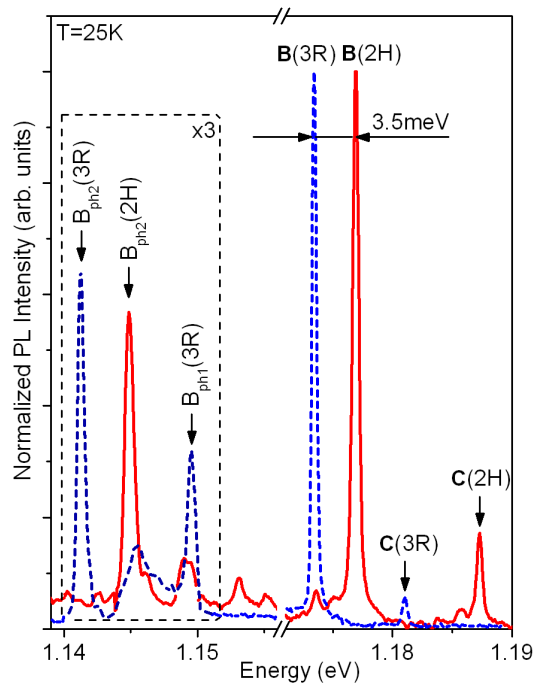


FIG. 1. (color online) Luminescent spectra at low temperature of Cl₂ intercalated 2H (blue broken line) and 3R (red solid line) MoS₂ single crystals.

depend on the absolute calibration of the spectrometer.

Fig. 2(a),(b) also shows that the 2H and 3R emission evolves in a qualitatively similar manner with temperature. For both polytypes the emission of exciton *C* gains in intensity with respect to the emission from exciton *B*. Quantitatively there are some differences. In contrast to 3R for which the exciton *B* emission dominates at all temperatures, in the 2H polytype the intensity ratio between *B* and *C* excitonic lines changes in favor of exciton *C* with increasing temperature. For both polytypes, increasing the temperature above 60K leads to a rapid quenching of all PL emission. Such a of the excitonic spectral lines in the case of 2H-MoS₂:Cl₂ crystals can be understood in terms of non-radiative transitions (phonon emission) which dominate over radiative recombination (photon emission) at higher temperatures.^{11,18} A common characteristic of the emission spectra for the both polytypes is that the excitonic region, very prominent at low temperatures, is accompanied by strong phonon replicas: $C_{ph1}-C_{ph3}$ and $B_{ph1}-B_{ph3}$ (see Fig. 2(a),(b)). The energies of the phonon replica emission are in good agreement with previous studies,¹¹ where they were interpreted as local phonon modes induced by the center at the origin of the exciton related luminescence.

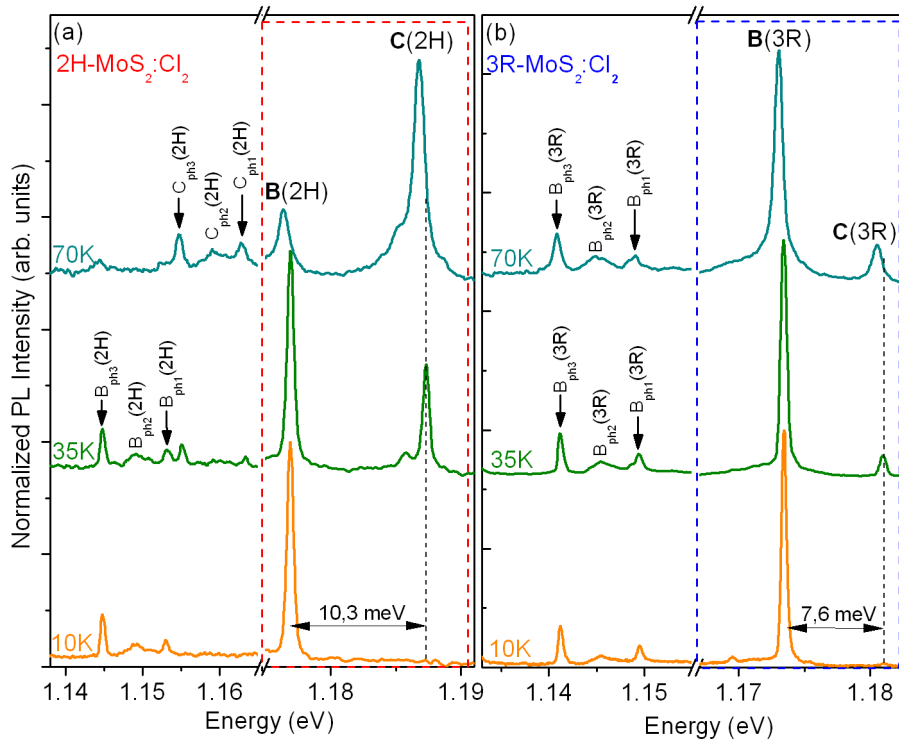


FIG. 2. (color online) PL spectra at different temperatures of (a) 2H-MoS₂ and (b) 3R-MoS₂ polytypes measured at different temperatures. The dashed vertical lines are a guide to the eye indicating the position of the weak *C* excitonic lines at 10K (which are nevertheless clearly visible in the *T* = 35 K spectra).

IV. MODEL DESCRIPTION

In order to explain the difference between 2H and 3R polytypes, we propose a model which describes the intercalation of halogen molecules in the two polytypes. As the X-ray single crystal study did not reveal any essential changes in the unit cell parameters in both studied polytypes, we have assumed the Cl₂ molecule is present in a relatively low concentration. In other words, we consider that the halogen molecules disturb the crystal lattice only locally. The intercalation of a considerable quantity of molecules should lead to a larger interlayer distance, compared to that in the pure phase; indeed such an increase of the inter-layers separation upon intercalation has been observed.^{13,19} Due to the lack of structural information concerning the position of the chlorine molecule, the DFT band structure calculations were carried out for the surfaces of 2H-MoS₂ and 3R-MoS₂ crystals. The studied surfaces were modeled by three molecular layers of polytypes that are without and with intercalation of Cl₂ molecules (model I and II respectively). For model I, three layers and corresponding atomic coordinates were taken from the structure of bulk crystals. In model II we assume that Cl₂ molecules are intercalated in the van der Waals gap only between two layers and move them apart while the other interlayer gap remains

unchanged.

Possible positions of Cl₂ molecules intercalated between MoS₂ layers were chosen on the basis of the bulk crystal structure analysis using PLATON tools.²⁰ The crystal packing of the layers revealed two types of interstitial cavities in the interlayer of the van der Waals gap. These cavities are similar in both polytypes and are formed by six or four surrounding sulphur atoms and have the shapes of a trigonal antiprism and a trigonal pyramid, respectively. The coordinates of corresponding centroids of these cavities are 0, 0, 0.5 and 2/3, 1/3, 0.561 in 2H-polytype and 2/3, 1/3, 0.167 and 1/3, 2/3, 0.208 in 3R-polytype. The shortest distance between the centroids of two such nearest cavities, which share a common face (three common sulphur atoms) equals 1.97Å in both polytypes. On the other hand a search of the Cambridge Structural Database (version 5.34)^{21,22} and Inorganic Crystal Structure Database²³ revealed that Cl - Cl distances in a chlorine molecule are between 1.96 and 1.98Å and that the shortest Cl - S inter molecular contacts in the crystal are in the range 3.29-3.31Å. Thus, the centroids of conjugate cavities are complementary to the chlorine molecule and this position obviously minimizes the necessary split of the interlayer of the van der Waals gap to adopt chlorine molecule taking into account the van der Waals size of these molecules and minimal possible Cl - S intermolecular distance.

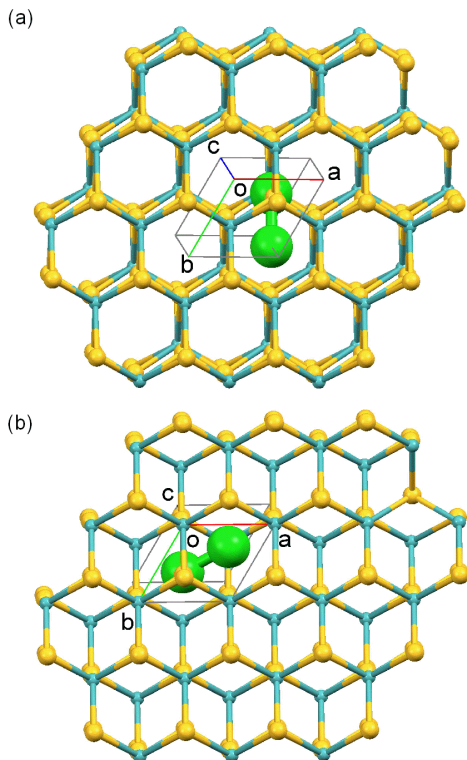


FIG. 3. (color online) (a), (b) Mutual arrangement of two neighbouring layers in the structure of 2H- (a) and 3R- (b) polytypes and position of Cl₂ molecule between these layers. View approximately along c crystallographic axis. Mo, S and Cl atoms are shown as spheres of arbitrary radii of cyan, yellow and green color, respectively.

To place Cl₂ molecules in the desired positions, the gap between two MoS₂ layers in model II was extended to provide the required Cl - S intermolecular distance. The separation between the planes of sulphur atoms from two neighboring MoS₂ layers was increased up to 6.083 and 6.279Å for the 2H- and 3R- polytypes, respectively, compared with the corresponding separation of 3.021 and 2.997Å in the bulky crystals and in model I. Although the chlorine molecule has a similar nearest neighbor surrounding, the further environment in polytypes differs due to unlike mutual arrangement of MoS₂ layers (Fig. 3(a), (b)). Even such small differences in halogen positions may affect the radiative properties of excitons bound to the halogen molecules, leading to distinct emission spectra.

Self-consistent ground-state calculations were performed with the ABINIT code²⁴ to obtain the detailed electronic structures. Electronic calculations were performed in the generalized gradient approximation with the Perdew-Burke-Ernzerhof exchange-correlation energy functional.²⁵

Orbitals are expanded in plane waves up to a cut-off of 25 Hartrees. The pseudo potentials used in our work

were generated from the pseudo potentials of Troullier-Martins.²⁶ The slab-model approach was used to construct the surface-induced bulk alignment of the crystals. In a slab model the super cell with the dimensions $3a \times 3b$ along the layers and parameter along c axis, which corresponds to three layers, were selected and repeated by use of periodic boundary conditions. When used with periodic basis functions (e.g., plane waves), the repetition is performed in three dimensions and a vacuum layer with the thickness of 10Å is introduced to isolate the slabs. Thus, the super cell always includes three MoS₂ layers for both 2H and 3R polytypes in models I and II. Only one chlorine molecule was introduced per super cell to model the low concentration. The $3a \times 3b$ dimension along the layer was chosen to perform calculations in reasonable computation time with available resources.

V. DISCUSSION

For bulk MoS₂, the electronic states near the Fermi level are dominated by Mo 4*d* and S 3*p* levels. Specifically, the conduction band states at the K point on the Brillouin zone, are primarily composed of strongly localized *d* orbitals at Mo atom sites. At the K point, the occupied part of the *d* band has dominant $d_{xy} - d_x^2 - y^2$ character whereas the unoccupied portion is dominated by d_z^2 character.²⁷ They have minimal interlayer coupling since Mo atoms are located in the middle of the S-Mo-S unit cell. The valence band maximum (VBM) is located at the Γ point while the conduction band minimum (CBM) is located about halfway between Γ and K points; the gap is thus indirect having a value of 1.28 eV. On the other hand, states near the Γ point originate from a linear combination of Mo d_z^2 orbitals and the S p_z orbitals and are fairly delocalized and have an antibonding nature. They have strong interlayer coupling and their energies depend sensitively on the layer thickness. As a consequence, increasing the separation between consecutive MoS₂ layers leads to weaker layer-layer interaction and lowers the energy of the antibonding states which causes the VBM to shift downwards. Thus, in the limit of widely separated planes, i.e., monolayer MoS₂, the material becomes a direct gap semiconductor with a gap of about 1.9eV at 300K.²⁸ Moreover, the stacking effect on the interlayer bonding was confirmed by the low energy diffraction study of MoS₂ single crystals,²⁹ which shows that the inter-plane distance between the Mo and S atomic planes within the topmost layer shrink about 5% compared to its bulk value. To resume, the electronic states at the Γ point are strongly affected by the long-range interlayer Coulombic interactions. In our case, halogen molecules intercalated within MoS₂ layers should influence the interlayer interaction especially at the Γ point. It should be not forgotten that the intercalation of any molecules between the layers leads to an enlargement of the adjacent layers, as was revealed in earlier publications.^{13,19} This interaction is more pronounced in the case of only

few MoS₂ layers as was suggested in.³⁰

This assumption is confirmed by our theoretical calculations of the electronic structure of the two polytypes with and without halogen intercalation, presented in Fig. 4. The model I has an indirect band gap structure, VBM being located at the Γ point while the CBM is located about halfway between Γ and K points. The values of indirect gaps are equal to 1.119 and 1.113 eV for 2H and 3R polytypes (Fig. 4 (a),(b)); the values for the gap of both polytypes are less than experimental ones but it is known that the density functional methodology underestimates the band gaps of semiconductors compared to the experimental results (in our calculations, which are not presented here, the E_g for these bulk materials were equal to 1.062 and 1.019eV respectively, which are also underestimated compared to experimental values). A similar band gap narrowing in 3R polytype, in comparison to that of 2H, was also observed in silicon carbide.³¹

Moreover, it was found for two single stacked sheets of MoS₂ that when the inter-sheet separation is greater than 4.5Å, the band gap reaches the value found for a single sheet, as the inter-sheet interaction vanishes.³² For both polytypes in our first model the number of layers is the same but the interlayer distances and stacking sequences are different. Within the stacking sequences ABAB for 2H-MoS₂ and ABCABC for 3R-MoS₂ the distances between the planes of sulphur atoms of neighboring S-Mo-S layers and distances between the planes of sulphur atoms within the same layer are 3.021, 2.997 and 3.129, 3.117Å, respectively. Moreover, in 3R-MoS₂ polytype the S-Mo-S layers are significantly shifted relatively each other in comparison with 2H-MoS₂ one (Fig. 3). Thus the structural features of these polytypes affect the long-range, interlayer Coulombic interactions which led to a difference in values of the band gaps.

In the second model for two polytypes the Cl₂ intercalation creates energy levels in the band gap near the conduction band edge which consist of $2p$ antibonding states of Cl atoms while the valence bands are comprised of d -electron orbitals of Mo atoms. Moreover, halogen intercalation completely changes the local band structure and the distribution of energy states over the Brillouin zone: both polytypes have now direct band gap transition at the Γ point with 1.323 and 1.246 eV values, for 2H and 3R polytypes, respectively (Fig. 4 (c),(d)). The values of halogen levels within the band gap of 2H and 3R polytypes are equal to 1.148 and 1.112 eV, respectively. The intercalation of Cl₂ molecule has led to widening of the band gaps compared to the band structure of the polytypes investigated in model I. The difference in the values of the given halogen levels is related to different positions of Cl₂ molecules between the layers where they have different spatial surrounding. For 2H-MoS₂, only one Cl atom in the molecule has a contact (4.32Å) with Mo atom (Fig. 3(a)) that is less than above the indicated threshold (4.5Å) when band gap does not depend on inter-layer separation. In contrast for 3R polytype,

the Cl atoms in the molecule have both contacts with the metals and they are less than in 2H polytype and equal to 4.279 and 4.316Å, respectively (Fig. 3(b)). Since in Cl₂ molecule the electrons are shared (not transferred), there are no existing ions that are positive or negative charges, which leads to the creation of full outer shells of chlorine atoms. This means that the repulsive forces hinder inter-layer coupling when Cl and Mo atoms are brought closer to each other, leading to a widening of the band gaps of the polytypes. In turn, that leads to a greater splitting of the antibonding states of Cl atoms in 3R-MoS₂, causing the lowering of the impurity levels in this polytype in comparison with 2H polytype. The band gap widening for both polytypes in model II in comparison with model I may be related to a long-range Coulombic interaction of chlorine molecules with the adjacent layers. For band structure calculation, molecules intercalated within MoS₂ layers increase the distance between the two layers. In order to understand the effect of halogen intercalation on the band structure transformation we calculated the energy bands for model II with increased distances but without Cl₂ (not presented here). The obtained values are equal to 1.319 and 1.248 eV for 2H and 3R polytypes respectively. These values are very similar to direct band gap transition at the Γ point in model II for 2H, 3R-MoS₂ which means that the intercalation of chlorine molecules have increased the distances between the adjacent layers which in turns have led to the local band gap widening.

Theoretical calculations have confirmed that the difference in halogen molecules positions in two polytypes should result in different PL spectra separated by a small amount of energy which, indeed, is observed experimentally. The temperature rise of the *C* peak in the luminescent spectra to the detriment of the *B* peak for 2H polytype occurs because the level responsible for the *C* emission peak has a radiative lifetime much shorter than the *B* level.¹⁸ In the case of 3R polytype, despite a smaller (in comparison with 3R polytype) distance between the *B* and *C* excitonic levels (7.5meV instead of 10.3meV), the temperature increase of the *C*-line relative intensity is unimportant. This indicates that the radiative lifetimes of these levels are not significantly different, and the relative intensity of lines *B* and *C* is determined mainly by their population (Boltzmann distribution). However, this approach should be confirmed experimentally by kinetic (time resolved) measurements, which will be the subject of a future publication.

VI. CONCLUSION

To summarize, the synthetic MoS₂ single crystals were grown by means of the CVT method using Cl₂ molecules as a transport agent. 2H-MoS₂ and 3R-MoS₂ polytypes were identified and structurally characterized using X-ray diffraction to determine its structure under intercalation of Cl₂ molecules. The absence of any changes of the unit cell parameters in both polytypes investigated indicates

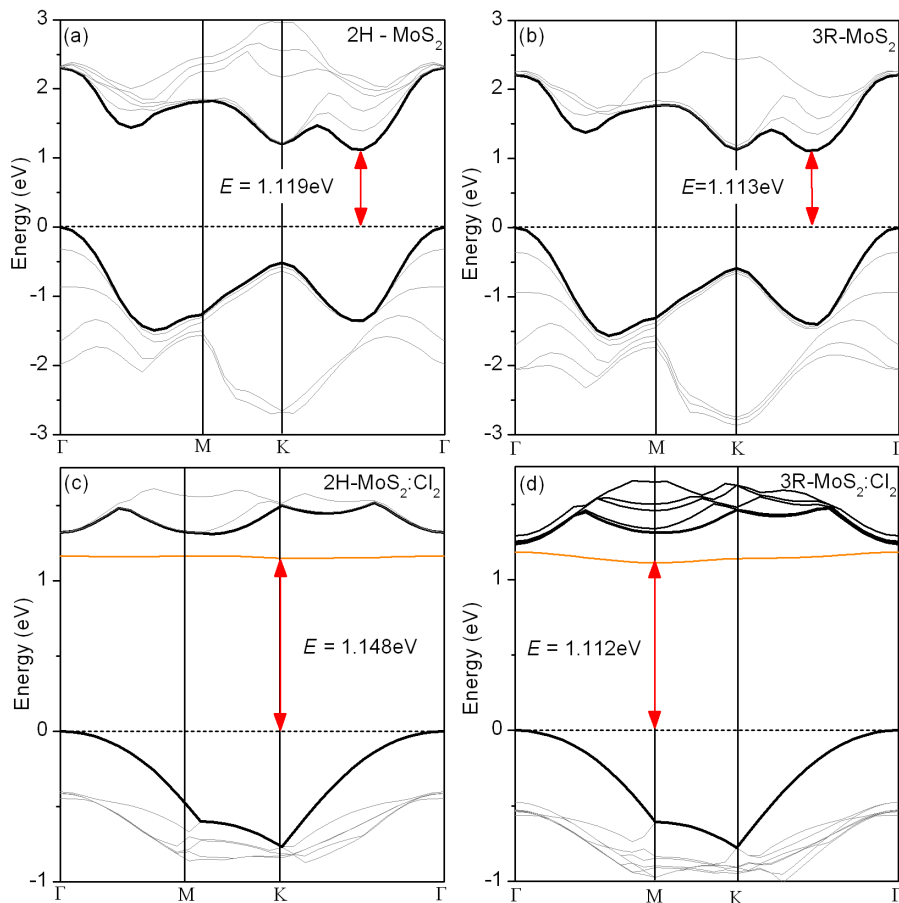


FIG. 4. (color online) Calculated electronic band structures of two models containing three layers of MoS₂. Band structures of 2H (a) and 3R (b) polytypes of MoS₂ where layers are fixed at bulk positions. Electronic band structure of halogen intercalated 2H (c) and 3R (d) polytypes of MoS₂. The orange line in (c) and (d) correspond to the halogen level within the band gap. The coordinates of k points in the Brillouin Zones in studied super cells are following: Γ : (0,0,0), M: (1/2,0,0), K: (1/3,1/3,0). The red arrows indicate the minimum energy value. The horizontal dashed lines indicate the valence band maximum.

that the concentration of Cl₂ molecules in the crystals is relatively low. Therefore, it was assumed that halogen molecules disturb the crystal lattice only locally because their intercalation in large concentration would have led to a larger interlayer distance in comparison to that in the pure phase. PL related to the excitons bound to the halogen molecules was investigated for the as grown 2H-MoS₂ and 3R-MoS₂ polytypes. It was shown that there is an evident difference between the low temperature luminescence spectra of the investigated polytypes: Notably the excitonic splitting is significantly different providing a robust signature of the polytype under investigation. The observed spectral shift and dissimilar behavior of the spectra as a function of temperature are explained as consequence of slightly different positions of halogen molecules in the interstitial space of the studied polytypes, which leads to a different interaction of the bound excitons with the local crystal field. To interpret the obtained experimental results the DFT band structure calculations were performed for three molecular lay-

ers of 2H-MoS₂ and 3R-MoS₂ polytypes without (model I) and with (model II) intercalation of Cl₂ molecules. For model II, the structural features of these polytypes were shown to affect the long-range interlayer Coulombic interactions, which led to a difference in values of the band gaps in 2H-MoS₂ and 3R-MoS₂ due to slightly different positions of halogen molecules in the interstitial space of these polytypes. The DFT band structure calculations for model II are in accordance with the spectroscopic experiments, i.e., that the halogen bounded excitonic spectra of 2H polytype are shifted to higher energies compared to those of 3R polytype. It was also shown that the halogen intercalation completely changes the local band structure and distribution of energy states over the Brillouin zone of both polytypes.

ACKNOWLEDGMENTS

We would like to thank Dr. Olga Iliasenco for technical assistance. The investigation has been carried out

in the framework of the HP-SEE project (the fast track access to HPC cluster resources available in the South-East Europe region) and of the STCU project Nr. 5809 (financial support for a part of the research).

-
- * angell@gmail.com
- ¹ C. Lee, Q. Li, W. Kalb, X.-Z. Liu, H. Berger, R. W. Carpick, and J. Hone, *Science* **328**, 76 (2010), <http://www.sciencemag.org/content/328/5974/76.full.pdf>.
 - ² D. Braga, I. Gutierrez Lezama, H. Berger, and A. F. Morpurgo, *Nano Letters* **12**, 5218 (2012), pMID: 22989251, <http://dx.doi.org/10.1021/nl302389d>.
 - ³ A. Splendiani, L. Sun, Y. Zhang, T. Li, J. Kim, C.-Y. Chim, G. Galli, and F. Wang, *Nano Letters* **10**, 1271 (2010), pMID: 20229981, <http://dx.doi.org/10.1021/nl903868w>.
 - ⁴ J. Puthussery, S. Seefeld, N. Berry, M. Gibbs, and M. Law, *Journal of the American Chemical Society* **133**, 716 (2011), pMID: 21175173, <http://dx.doi.org/10.1021/ja1096368>.
 - ⁵ K. S. Novoselov, D. Jiang, F. Schedin, T. J. Booth, V. V. Khotkevich, S. V. Morozov, and A. K. Geim, *Proceedings of the National Academy of Sciences of the United States of America* **102**, 10451 (2005), <http://www.pnas.org/content/102/30/10451.full.pdf+html>.
 - ⁶ M. Bougouma, A. Batan, B. Guel, T. Segato, J. B. Legma, F. Reniers, M.-P. Delplancke-Ogletree, C. Buess-Herman, and T. Doneux, *Journal of Crystal Growth* **363**, 122 (2013).
 - ⁷ K. K. Tiong and T. S. Shou, *Journal of Physics: Condensed Matter* **12**, 5043 (2000).
 - ⁸ S. Hu, C. Liang, K. Tiong, Y. Lee, and Y. Huang, *Journal of Crystal Growth* **285**, 408 (2005).
 - ⁹ R. Suzuki, M. Sakano, Y. J. Zhang, R. Akashi, D. Morikawa, A. Harasawa, K. Yaji, K. Kuroda, K. Miyamoto, T. Okuda, K. Ishizaka, R. Arita, and Y. Iwasa, *Nat Nano* **9**, 611 (2014), <http://dx.doi.org/10.1038/nnano.2014.148>.
 - ¹⁰ L. Kulyuk, E. Bucher, L. Charron, E. Fortin, A. Nateprov, and O. Schenker, *Nonlinear Optics (Mlc) Section B* **29**, 501 (2002).
 - ¹¹ L. Kulyuk, L. Charron, and E. Fortin, *Phys. Rev. B* **68**, 075314 (2003).
 - ¹² L. Kulyuk, D. Dumcehnko, E. Bucher, K. Friemelt, O. Schenker, L. Charron, E. Fortin, and T. Dumouchel, *Phys. Rev. B* **72**, 075336 (2005).
 - ¹³ D. D'Ambra, J. Marzik, R. Kershaw, J. Baglio, K. Dwight, and A. Wold, *Journal of Solid State Chemistry* **57**, 351 (1985).
 - ¹⁴ J. Baglio, E. Kamieniecki, N. DeCola, C. Struck, J. Marzik, K. Dwight, and A. Wold, *Journal of Solid State Chemistry* **49**, 166 (1983).
 - ¹⁵ R. C. Clark and J. S. Reid, *Acta Crystallographica Section A* **51**, 887 (1995).
 - ¹⁶ G. M. Sheldrick, *Acta Crystallographica Section A* **64**, 112 (2008).
 - ¹⁷ B. Schnfeld, J. J. Huang, and S. C. Moss, *Acta Crystallographica Section B* **39**, 404 (1983).
 - ¹⁸ A. Colev, C. Gherman, V. Mirovitskii, L. Kulyuk, and E. Fortin, *Journal of Luminescence* **129**, 1945 (2009), special Issue based on The 15th International Conference on Luminescence and Optical Spectroscopy of Condensed Matter (ICL'08).
 - ¹⁹ E. Benavente, M. S. Ana, F. Mendizbal, and G. Gonzalez, *Coordination Chemistry Reviews* **224**, 87 (2002).
 - ²⁰ A. L. Spek, *Journal of Applied Crystallography* **36**, 7 (2003).
 - ²¹ I. J. Bruno, J. C. Cole, P. R. Edgington, M. Kessler, C. F. Macrae, P. McCabe, J. Pearson, and R. Taylor, *Acta Crystallographica Section B* **58**, 389 (2002).
 - ²² F. H. Allen, *Acta Crystallographica Section B* **58**, 380 (2002).
 - ²³ A. Belsky, M. Hellenbrandt, V. L. Karen, and P. Luksch, *Acta Crystallographica Section B* **58**, 364 (2002).
 - ²⁴ X. Gonze, J.-M. Beuken, R. Caracas, F. Detraux, M. Fuchs, G.-M. Rignanese, L. Sindic, M. Verstraete, G. Zerah, F. Jollet, M. Torrent, A. Roy, M. Mikami, P. Ghosez, J.-Y. Raty, and D. Allan, *Computational Materials Science* **25**, 478 (2002).
 - ²⁵ J. P. Perdew, K. Burke, and M. Ernzerhof, *Phys. Rev. Lett.* **77**, 3865 (1996).
 - ²⁶ N. Troullier and J. L. Martins, *Phys. Rev. B* **43**, 1993 (1991).
 - ²⁷ A. Ramasubramaniam, D. Naveh, and E. Towe, *Phys. Rev. B* **84**, 205325 (2011).
 - ²⁸ A. H. Reshak and S. Auluck, *Phys. Rev. B* **71**, 155114 (2005).
 - ²⁹ B. J. Mrstik, R. Kaplan, T. L. Reinecke, M. Van Hove, and S. Y. Tong, *Phys. Rev. B* **15**, 897 (1977).
 - ³⁰ J. K. Ellis, M. J. Lucero, and G. E. Scuseria, *Applied Physics Letters* **99**, 261908 (2011).
 - ³¹ W. R. L. Lambrecht, S. Limpijumngong, S. N. Rashkeev, and B. Segall, *physica status solidi (b)* **202**, 5 (1997).
 - ³² T. Li and G. Galli, *The Journal of Physical Chemistry C* **111**, 16192 (2007), <http://dx.doi.org/10.1021/jp075424v>.